Journal of Molecular Structure 1314 (2024) 138818

Contents lists available at ScienceDirect

Journal of Molecular Structure

journal homepage: www.elsevier.com/locate/molstr

Synthesis, characterisation, X-ray diffraction and biological evaluation of new thiourea derivatives against *Mycobacterium tuberculosis and* cervical cancer

Luleka Makhakhayi [a], Frederick P. Malan [b], Sibusiso Senzani [c], Matshawandile Tukulula [d], Candace Davison [e], Jo-Anne de la Mare [e], Comfort M. Nkambule [a], Vuyelwa J. Tembu [a], Amanda-Lee E. Manicum [a,*]

[a] *Department of Chemistry, Tshwane University of Technology, Pretoria 0001, South Africa*
[b] *Department of Chemistry, University of Pretoria, Pretoria 0001, South Africa*
[c] *School of Laboratory Medicine and Medical Science, University of KwaZulu Natal, Durban 4001, South Africa*
[d] *School of Chemistry and Physics, University of KwaZulu Natal, Durban 4001, South Africa*
[e] *Department of Biochemistry and Microbiology, Female Cancers Research at Rhodes University (FemCR2U), Makhanda/Grahamstown, 6140, South Africa*

ARTICLE INFO

Keywords:
Anticancer
Antimycobacterial
Antitubercular
S,O-bidentate ligands
Thiourea

ABSTRACT

In this study, thiourea derivatives were prepared to identify potentially effective compounds against tuberculosis and cervical cancer. The newly synthesized compounds, namely *N-(cyclohexyl(methyl)carbomothioyl) benzamide* (**TU1**), *N-(cyclohexyl(methyl)carbamothioyl)-2-methylbenzamide* (**TU2**), *N-(*dicyclohexylcarbamothioyl*) benzamide (***TU3***), N-(dicyclohexylcarbamothioyl)-4-nitrobenzamide* (**TU4**), *N-(diphenylcarbamothioyl) benzamide* (**TU5**), and *N-(diphenylcarbamothioyl)-4-nitrobenzamide* (**TU6**), were obtained in high purity and yields. The compounds were successfully characterized by infrared spectroscopy (IR), ultraviolet-visible spectroscopy (UV-Vis), nuclear magnetic resonance (NMR), single crystal X-ray diffractometer (SCXRD), mass spectrometry (MS) and the melting points (mp). Crystal structure analyses of **TU1, TU2** and **TU6** were carried out which showed, that in the solid state, the molecules were linked together by intermolecular hydrogen bonds, specifically N—H···S and C—H···O interactions. *In-vitro* testing against *M. tuberculosis (Mtb)* revealed compounds **TU1** and **TU2** to be the most potent with MIC_{90} values of 28.2 and 11.2 μM, respectively. However, compounds **TU4, TU5**, and **TU6**, with MIC_{90} values of 80.3, 82.8 and 107.7 μM, respectively, exhibit mild antituberculosis activity, whereas **TU3** with a MIC_{90} value of 752.7 μM is considered inactive against the *Mtb* strain. None of the compounds demonstrated significant selectivity for bacterial cells versus human cells and thus further studies could be dedicated to creating derivatives of **TU1** and **TU2** that are more selective. *In vitro* biological screening against HeLa cells revealed two highly toxic compounds, **TU2** and **TU6,** with respective IC_{50} values of 12.00 ± 1.21 **μM** (SI = 1.06) and 8.45 ± 1.21 μM (SI = 0.08); and two moderately toxic compounds, **TU4** (IC_{50} = 27.75 ± 1.15 μM; SI = 0.35) and **TU5** (IC_{50} = 23.66 ± 1.24 μM; SI = 0.29).

1. Introduction

Thiourea, also known as thiocarbamide, is an organosulfur compound with the chemical formula (R_1R_2N) (R_3R_4N) C═S. Thioureas act as chelating agents [1–4] and have found extensive applications in the field of medicines and analytical chemistry ([5,6]) Its derivatives have demonstrated significant versatility in various academic, pharmacological, industrial, biological, commercial, and agricultural applications ([7,8]). Due to their distinctive chemical properties, these compounds can be readily altered as ligands, significantly enhancing their bioactivity. These compounds also exhibit a wide range of biological activities, including but not limited to their use as anaesthetics agents [9], anticarcinogens ([10,11]), anticonvulsants [12], and antitubercular agents [13].

Tuberculosis, commonly referred to as TB, is an infectious bacterial disease caused by *Mycobacterium tuberculosis (*Mtb*)*. It primarily affects

* Corresponding author.
E-mail address: ManicumAE@tut.ac.za (A.-L.E. Manicum).

https://doi.org/10.1016/j.molstruc.2024.138818
Received 11 October 2023; Received in revised form 28 May 2024; Accepted 29 May 2024
Available online 30 May 2024

the lungs, considered the primary sites, and subsequently disseminates through the circulatory and lymphatic systems to other secondary sites such as the liver, bones, spleen, and joints [14–16]. TB is one of the top ten causes of mortality and a primary contributor among HIV-positive individuals. According to the World Health Organization (WHO) report, a large number of deaths worldwide are a result of the spread of TB disease caused by a single infectious bacterium. Despite the availability of various commercial anti-TB drugs, the disease continues to kill a large number of people around the world. Furthermore, it has been reported that approximately 74 million lives were saved through TB diagnosis and treatment between the years 2000 and 2021 [17–19]. The management of tuberculosis requires the administration of several antibiotics over an extended duration, which may result in antibiotic resistance [20]. This is a significant challenge that becomes more pronounced as the prevalence of multiple drug-resistant tuberculosis (MDR-TB) rises. Typically, longer treatment duration is associated with the occurrence of side effects and the complexity of the drug regimen needs to be increased [21–23]. Although new anti-TB medications [24], such as bedaquiline [25] and delamanid [26] (as shown in Fig. 1), have been approved, some anti-TB drugs also affect the host's immune system while killing *Mycobacteriaceae* pathogenic bacteria. Therefore, there is an urgent need for novel therapeutic agents with reduced toxicity profiles to tackle the proliferation of tuberculosis.

In the present study, we report the synthesis, characterization (IR, NMR, MS, UV-Vis), and crystallography studies for six thiourea ligands namely; *N*-(cyclohexyl(methyl)carbomothioyl) benzamide (**TU1**), *N*-(cyclohexyl(methyl)carbamothioyl)-2-methylbenzamide (**TU2**), *N*-(dicyclohexylcarbamothioyl)benzamide (**TU3**), *N*-(dicyclohexylcarbamothioyl)-4-nitrobenzamide (**TU4**), *N*-(diphenylcarbamothioyl) benzamide (**TU5**), and *N*-(diphenylcarbamothioyl)-4-nitrobenzamide (**TU6**). The single crystal structure analysis of **TU1, TU2** and **TU6** were also performed. The synthesis and characterization data are enriched by the *in vitro* antimycobacterial studies against the H37RV *M. tuberculosis* strain and cytotoxicity studies in human cells including the HeLa cervical cancer cell line and MCF12A non-tumorigenic breast epithelial cell line. There is a possibility that thiourea derivatives may be more effective as antimicrobial and anticancer agents. However, there is still a need for a comprehensive investigation relating to the structure and the activity of thiourea derivatives as well as their stability under biological conditions.

2. Experimental

2.1. Material and measurements

Unless specified otherwise, analytical reagents used for the preparation and characterization of compounds were bought from Sigma Aldrich and Strem Chemicals. Solvents and reagents utilized for synthetic purposes were used as received without any additional purification, except when drying was necessary. All reagents or chemical reactions that required anaerobic or oxygen-free conditions were performed using argon or nitrogen gas. For infrared characterization, PerkinElmer spectrometer spectrum Two (UATR Two) was used to record the absorption of the compound. The IR is coupled to a computer and is equipped with a temperature cell regulator (accurate to 0.3 °C). All the infrared spectra of synthesized compounds were recorded at room temperature and solid samples were analysed. IR absorption was recorded in wave number (cm^{-1}) on KBr pellets between 4000 and 400 cm^{-1}. All the NMR data were obtained from a Varian Gemini400 (operating at 400 and 100 MHz for ^{1}H and ^{13}C, respectively) spectrometer at room temperature, using acetone (D_6) as the solvent. The chemical shifts (δ) are reported in ppm with ^{1}H and ^{13}C spectra primarily calibrated relative to the residual deuterated solvents acetone-d_6 (δ_H = 2.05 and δ_c = 29.8; 206.3 ppm). All coupling constants (*J*) are reported in Hertz (Hz). A PerkinElmer Lambda XLS+ Ultra-violet/Visible (UV/Vis) spectrometer was used to collect UV/Vis data in methanol solvent, using a 1.000 ± 0.001 cm quartz cuvette cell. Waters Synapt G2, ESI probe, ESI Pos, and Cone Voltage 15 V were used for the determination of quasi molecular ion, MS.

2.2. General procedure for the synthesis of thiourea ligands

The ammonium thiocyanate (17 mmol) was dissolved in hot acetone (10 mL) and the substituted benzoyl chloride (17 mmol, R = H, NO_2, CH_3) was added dropwise while stirring. The reaction mixture was filtered after 20 min, and the carbonyl isothiocyanate filtrate was collected and heated at 65 °C for 30 min [27,28]. Thereafter, solutions of 3 x secondary amine (*N*-methylcyclohexylamine, dicyclohexylamine, diphenylamine) were added slowly to the heated carbonyl isothiocyanate, as shown in Scheme 1. The resultant reaction mixtures were allowed to stir for 30 min at room temperature. On completion, as confirmed by TLC, the thiourea ligands were precipitated with distilled water, collected by filtration, and washed with water. The final products were then recrystallized from *n*-hexane and ethyl acetate solutions (7:3) and obtained yields ranging from 73 to 89 %.

N-(cyclohexyl(methyl)carbomothioyl) benzamide [**TU1**]: White crystals. Yield: 73 %. m.p.: 145.9-146.8 °C IR: ν_{max} (cm^{-1}) = 3317 (N—H), 2929 (C—H_{asym}), 2855 (C—H_{sym}), 1682 (C═O), 1287 (C—N), 1140 (C═S), 1086, 1077 and 1044 (C—N). ^{1}H NMR (Acetone-d_6, 400 MHz, ppm): δ_H 9.49 (s, 1H), 8.01 (d, *J* = 7.1 Hz, 2H), 7.60 (t, *J* = 1.3 Hz, 3H), 3.33 (s, 2H), 1.72 – 1.49 (m, 4H), 1.41 (q, *J* = 13.0 Hz, 3H), 1.24 (t, *J* = 13.1 Hz, 2H). ^{13}C NMR (Acetone-d_6,100 MHz, ppm): δ_c 181.2, 164.2, 134.2, 133.3, 129.4, 129.1, 128.9, 63.2, 36.5, 34.8, 30.8, 29.6, 26.4. UV-Vis (CH_3OH): ε (λ_{max} = 223 nm) = 1497 $M^{-1}cm^{-1}$. HRMS (ES^{+}): 277.1385 $[M + H]^{+}$ (found), 276.1296 (calculated from $C_{15}H_{20}N_2OS$).

N-(cyclohexyl(methyl)carbamothioyl)-2-methylbenzamide [**TU2**]:

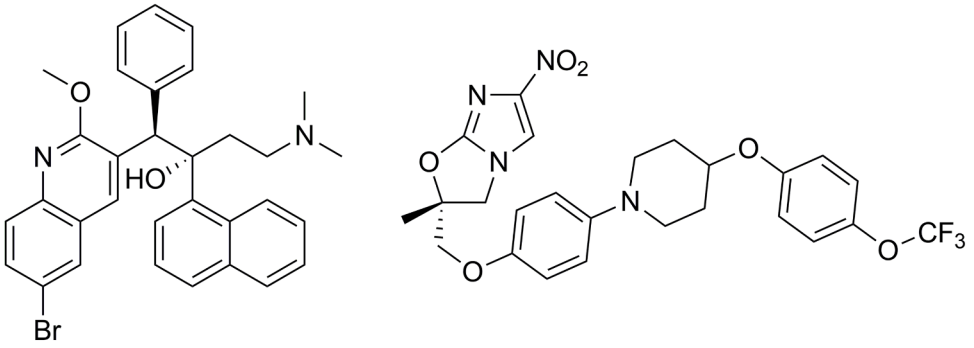

Bedaquiline Delamanid

Fig. 1. Structures of new approved anti-TB drugs ([25,26]).

White crystals. Yield: 89 %. m.p.: 156.0-156.9 °C. IR: ν_{max} (cm^{-1}) = 3258 (N-H), 2932 (C-H_{asym}), 2860 (C-H_{sym}), 1689 (C═O), 1284 (C—N), 1179 (C═S), 1084, 1069 and 1043 (C—N). ^{1}H NMR (Acetone-d_6, 400 MHz): δ 8.79 (s,1H), 7.23 (d, J = 7.8 Hz, 1H), 7.06 (td, J = 7.5, 1.5 Hz, 1H), 6.94 (dd, J = 13.7, 7.3 Hz, 2H), 2.99 (s, 3H), 2.21 (s, 3H), 2.10 (s, 1H), 1.69 (d, J = 56.0 Hz, 2H), 1.55 – 1.26 (m, 4H), 1.26 (qd, J = 12.3, 3.8 Hz, 2H), 1.11 (dd, J = 14.1, 4.9 Hz, 1H). ^{13}C NMR (Acetone-d_6,100 MHz, ppm): δ 180.8, 166.3, 137.8, 136.1, 131.8, 131.2, 128.6, 126.5, 63.1, 36.5, 35.0, 30.8, 26.6, 26.2, 25.2, 20.2. UV-Vis (CH_3OH): ε (λ_{max} = 228 nm) = 1281.4 $M^{-1}cm^{-1}$. HRMS (ES^+): 291.1531 [M + H] $^+$, (found), 290.1453 (calculated from $C_{16}H_{22}N_2OS$).

*N-(*dicyclohexylcarbamothioyl*) benzamide* [**TU3**]: Yellow crystals. Yield: 81 %. m.p.: 151.4-152.2 °C. IR: ν_{max} (cm^{-1}) = 3261 (N-H), 2928 (C-H_{asym}), 2852 (C-H_{sym}), 1688 (C═O), 1288 (C—N), 1143 (C═S), 1070, 1042 and 1038 (C—N). ^{1}H NMR (Acetone-d_6, 400 MHz, ppm): δ 9.03 (s,1H) 8.06 – 7.98 (m, 3H), 7.56 – 7.48 (m, 3H), 1.89 (s, 1H), 1.85 – 1.72 (m, 10H), 1.67 – 1.57 (m, 4H), 1.34 (s, 3H), 1.25 – 1.10 (m, 4H). ^{13}C NMR (Acetone-d_6,100 MHz, ppm): δ 182.4, 165.9, 134.8, 133.0, 132.8, 129.4, 129.1, 128.8, 54.1, 31.4, 30.6, 26.8, 26.2, 26.1, 25.4. UV-Vis (CH_3OH): ε (λ_{max} = 243 nm) = 4084.3 $M^{-1}cm^{-1}$. HRMS (ES^+): 345.2015 [M + H]$^+$, (found), 344.1922 (calculated from $C_{20}H_{28}N_2OS$).

N-(dicyclohexylcarbamothioyl)-4-nitrobenzamide [**TU4**]: Yellow crystals. Yield: 89 %. m.p.: 154.7–155.2 °C. IR: ν_{max} (cm^{-1}) = 3350 (NH), 2978 (C-H_{asym}), 2865 (C-H_{sym}), 1690 (C═O), 1540 (Ar-NO_2 asym), 1364 (Ar-NO_2 sym), 1290 (C—N), 1166 (C═S), 1088, 1169 and 1056 (C—N). ^{1}H NMR (Acetone-d_6, 400 MHz, ppm): δ 8.03 (s.1H), 8.00 (d, J = 17.8 Hz, 2H), 7.88 (m, 3H), 3.06 – 2.86 (m, 2H), 1.88-177 (m, 3H), 1.57 (d, J = 8.5 Hz, 5H), 1.41 (dt, J = 12.6, 3.6 Hz, 3H), 1.22 (td, J = 11.4, 10.4, 2.6 Hz, 3H), 1.21 – 1.14 (m, 4H), 1.01 – 0.94 (m, 2H). ^{13}C NMR (Acetone-d_6,100 MHz, ppm): δ 182.4, 166.0, 151.5, 139.1, 134.8, 133.1, 130.4, 129.7, 129.4, 128.8, 54.1, 31.2, 30.6, 26.7, 26.1, 25.3. UV-Vis (CH_3OH): ε (λmax = 228 nm) = 1251.7 $M^{-1}cm^{-1}$. HRMS (ES^+): 390.1861 [M + H]$^+$, (found), 389.1773 (calculated from $C_{20}H_{27}N_3O_3S$).

N-(diphenylcarbamothioyl) benzamide [**TU5**]: Yellow crystals. Yield: 85 %. m.p.:154.3-155.2 °C. IR: ν_{max} (cm^{-1}) = 3224 (N-H), 2931 (C-H_{asym}), 2854 (C-H_{sym}), 1690 (C═O), 1283 (C—N), 1184 (C═S), 1083, 1054 and 1038 (C—N). ^{1}H NMR (Acetone-d_6, 400 MHz, ppm): δ 9.99 (s, 1H), 7.86 – 7.70 (m, 2H), 7.65 – 7.47 (m, 1H), 7.34 (m, 9H), 7.26 – 7.12 (m, 3H). ^{13}C NMR (Acetone-d_6,100 MHz, ppm): δ 184.2, 163.1, 146.3, 143.8, 135.4, 133.3, 133.2, 132.3, 132.3, 130.3, 129.3, 129.1, 129.0, 128.3, 128.0, 127.1, 126.9, 120.1, 117.2. UV-Vis (CH_3OH): ε (λ_{max} = 220 nm) = 4188.3 $M^{-1}cm^{-1}$. HRMS (ES^+): 333.1068 [M + H]$^+$, (found), 332.0983 (calculated from $C_{20}H_{16}N_2OS$).

N-(diphenylcarbamothioyl)-4-nitrobenzamide [**TU6**]: Yellow crystals. Yield: 79 %. m.p.: 156.3-157.2 °C. IR: ν_{max} (cm^{-1}) = 3286 (NH), 2944 (C-H_{asym}), 2876 (C-H_{sym}), 1689 (C═O), 1533 (Ar-NO_2 asym), 1356 (Ar-NO_2 sym), 1279 (C—N), 1134 (C═S), 1092, 1064 and 1058 (C—N). ^{1}H NMR (Acetone-d_6, 400 MHz, ppm): δ 8.46 (s, 1H), 8.31– 8.19 (m, 2H), 8.17 (d, J = 8.4 Hz, 2H), 8.11 (d, J = 8.4 Hz, 2H), 7.99 – 7.69 (d, J = 7.5 Hz, 3H), 7.52 (d, J = 7.3 Hz, 3H), 7.46 – 7.10 (m, 2H). ^{13}C NMR (Acetone-d_6,100 MHz, ppm): δ 184.2, 162.6, 151.0, 147.0, 139.6, 131.2, 130.8, 130.6, 130.0, 129.7, 128.7, 128.0, 127.1, 126.8, 125.5, 124.6, 124.3, 123.9, 121.0, 118.0. UV-Vis (CH_3OH): ε (λ_{max} = 225 nm) = 1087 $M^{-1}cm^{-1}$. HRMS (ES^+): 378.0912 [M + H]$^+$, (found), 377.0834 (calculated from $C_{20}H_{15}N_3O_3S$).

2.3. Single-crystal X-ray crystallography

Single crystals of **TU1, TU2,** and **TU6** were analysed on a Rigaku XtaLAB Synergy R diffractometer [29], with a rotating-anode Mo/Cu X-ray source and a HyPix CCD detector. Data reduction and absorption were carried out using the CrysAlisPro (version 1.171.40.23a) software package. All X-ray diffraction measurements were performed at 150.0 (2) K, using an Oxford Cryogenics Cryostat. All structures were solved by direct methods with SHELXT-2013 [30] using the OLEX2 [31] interface. For data collection and refinement parameters, see Table 1. The

Table 1
Crystal data and structure refinement for **TU1, TU2**, and **TU6**.

Crystallographic data	(TU1)	(TU2)	(TU6)
Empirical formula	$C_{15}H_{20}N_2OS$	$C_{16}H_{22}N_2OS$	$C_{20}H_{15}N_3O_3S$
Formula weight (g.mol^{-1})	275.38	290.15	377.4
Temperature (K)	150.0(2)	150.0(2)	150.0(2)
Wavelength (Å)	1.54184	0.71073	0.71073
Crystal system	Monoclinic	Monoclinic	Triclinic
Space group	P21/c	P21/c	P-1
a (Å)	5.531(10)	7.9426(3)	6.8186(2)
b (Å)	13.514(2)	23.3394(5)	10.03181(2)
c (Å)	19.571(3)	8.9398(3)	13.2816(3)
α (°)	90	90	89.529(2)
β (°)	94.76(10)	112.789(4)	78.134(2)
γ (°)	90	90	89.102(2)
Volume(Å3)	1457.86(4)	1527.85(9)	888.96(4)
Z	4	4	2
ρcalc (g.cm^{-3})	1.255	1.308	1.406
μ (mm^{-1})	1.915	0.283	0.209
F (000)	588	640	390
θ range ()	3.986-78.810	2.621-30.752	2.559-30.941
Index ranges	$-7 \le h \le 5$	$-10 \le h \le 9$	$-8 \le h \le 8$
	$-16 \le k \le 16$	$-33 \le k \le 28$	$-13 \le k \le 10$
	$-24 \le l \le 24$	$-12 \le l \le 12$	$-16 \le l \le 17$
Reflections collected	17873	21251	10698
Reflections with I > 2σ(I)	3 043	4025	4318
Rint	0.0430	0.0300	0.0303
Completeness %	99.8	100	98.7
Data/restraints/parameters	3043/0/172	4025/0/183	4318/0/244
GooF	1.066	1.054	1.071
R [I > 2σ(I)]	R1 = 0.0488	R1 = 0.0351	R1 = 0.0389
	wR2 = 0.1355	wR2 = 0.0880	wR2 = 0.0945
R (all data)	R1 = 0.0528	R1 = 0.0414	R1 = 0.0500
	wR2 = 0.1385	wR2 = 0.0909	wR2 = 0.1002
Largest diff. peak and hole (e. $Å^{-3}$)	0839 and -0.510	0.389 and -0.447	0.358 and -0.364

DIAMOND [32] and Mercury [33] software were utilized to obtain the molecular visual depiction of the crystal structures. Thermal ellipsoids, depicting structures, are presented at a 50 % probability. The anisotropic refinement was applied to all atoms except for hydrogen, which had its isotropic displacement parameters fixed at U_{iso} (H) = 1.2 Ueq I, allowing them to ride on the parent atom. The X-ray crystallographic coordinates for all structures have been deposited at the Cambridge Crystallographic Data Centre (CCDC), with deposition numbers CCDC-2298808 (**TU1**), CCDC-2295487 (**TU2**), CCDC-2298807 (**TU6**). The data can be obtained free of charge from The Cambridge Crystallographic Data Centre via www.ccdc.cam.ac.uk/data_request/cif.

2.4. Antimycobacterial assay

The antimicrobial activity of the various compounds against the H37Rv strain of *M. tuberculosis* was tested in triplicate using microbroth dilution assays. Microtiter plates were then set up using 96 well plates containing 12 rows. Antibiotic stocks containing 4 × the initial concentration (4 mg/mL) required for the first row in the plate were set up, and 100 μL of the stock was inoculated into the first row. Thereafter, 50 μL of media was inoculated into rows 2 to 12, then a 50 μL aliquot of the antibiotic stock from row 1 was inoculated into row 2, mixed, and 50 μL was removed from row 2 and inoculated into row 3. This was done through to row 12, and a 50 μL aliquot was removed from the last row and discarded.

The inoculum was diluted 10-fold, and a 50 μL aliquot was added to each well. These plates were sealed and incubated at 37 °C for 14 days. Following this, 30 μL of a 0.02 % resazurin solution was aliquoted into each well, after which the plates were incubated at 37 °C overnight. Microbial growth was measured by observing the resazurin colour change from blue to pink. In addition to the compounds tested, Ethambutol was included as a positive control, and broth and solvent as negative controls. The 90 % minimum inhibitory concentration (MIC_{90})

was interpreted as the lowest concentration inhibiting a colour change from blue to pink [34].

2.5. Resazurin assay

A resazurin assay was used to determine cell viability and the IC_{50} values of the compounds, in the HeLa cervical cancer cell line (ATCC CCL-22), and a non-tumorigenic breast epithelial `cell line MCF12A (ATCC: CRL-10782). The cells were seeded at a density of 5000 cells/well in a 96-well plate and allowed to attach overnight at 37 °C and 9 % CO_2 in a humidified incubator. The cells were then treated for 96 h at a concentration range of 15.63 to 500.00 μM. Resazurin (0.54 μM) was added to the wells and the cells were incubated for 2–4 h at 37 °C in 9 % CO_2. Fluorescence readings were obtained on a Spectramax spectrophotometer (excitation and emission wavelength set at 560 nm and 590 nm, respectively) ([35,36]). The assay was performed in triplicate and the data was analysed using GraphPad Prism Inc., (USA) with half-maximal inhibitory concentration (IC_{50} values) determined by non-linear regression. Selectivity indices were calculated as the ratio of IC50 values in the human cell line over that of the MIC90 against Mtb, where a value of 1 indicates that compounds are equally toxic to human and Mtb cells, and a value >1 indicates selectivity for human cells over Mtb, where an SI > 2 is preferred in terms of true selectivity.

3. Results and discussions

3.1. Single crystal X-ray studies

Single crystals were obtained by slow evaporation of a methanol solution of **TU1, TU2** and **TU6** yielding the subsequent molecular structures . The molecular structures of the titled compounds are shown in Fig. 2, bond length, bond angles and torsion angles are given in Table 2 and hydrogen bonds in Table 3.

The bond lengths and angles are normal and agree with those expected from the thiourea derivatives ([37,38]). The bond length of O1—C1 and S1—C2 shows a typical double bond character with the bond length of 1.216(2), 1.218(14) 1.214(18) Å, and 1.680(2), 1.677 (11), 1.666(13) Å, for **TU1, TU2** and **TU6**, respectively. The C—N bond lengths of the compound are all shorter than the average single C—N bond length, which is C2—N1 = 1.331(2), 1.328(14), 1.349(17) Å, C3—N1 = 1.465(3), 1.468(14), 1.228(17) Å, C1—N2 = 1.388(2), 1.385 (14), 1.389(17) Å and C2—N2 = 1.401(2), 1.405(14), 1.395(17) Å for **TU1, TU2** and **TU6**, respectively as shown in Table 2. This shows different degrees of single-bond characters. The elongation of C2—N2 relative to C2—N1 corresponds to other reported thiourea derivatives ([37,38–45]) and is due to the electron-withdrawing effect on the carbonyl group. The bond angles of O1—C1—N2 are 123.78(18), 121.75(11) and 122.99(12) ° for **TU1, TU2** and **TU6** respectively, whereas the thiocarbonyl bond angles for N2—C2—S1 are 117.77(14), 117.58(8) and 120.35(10) ° and for N1—C2—S1 are 125.45(15), 125.90 (9) and 123.60(10) ° for **TU1, TU2** and **TU6** respectively, which

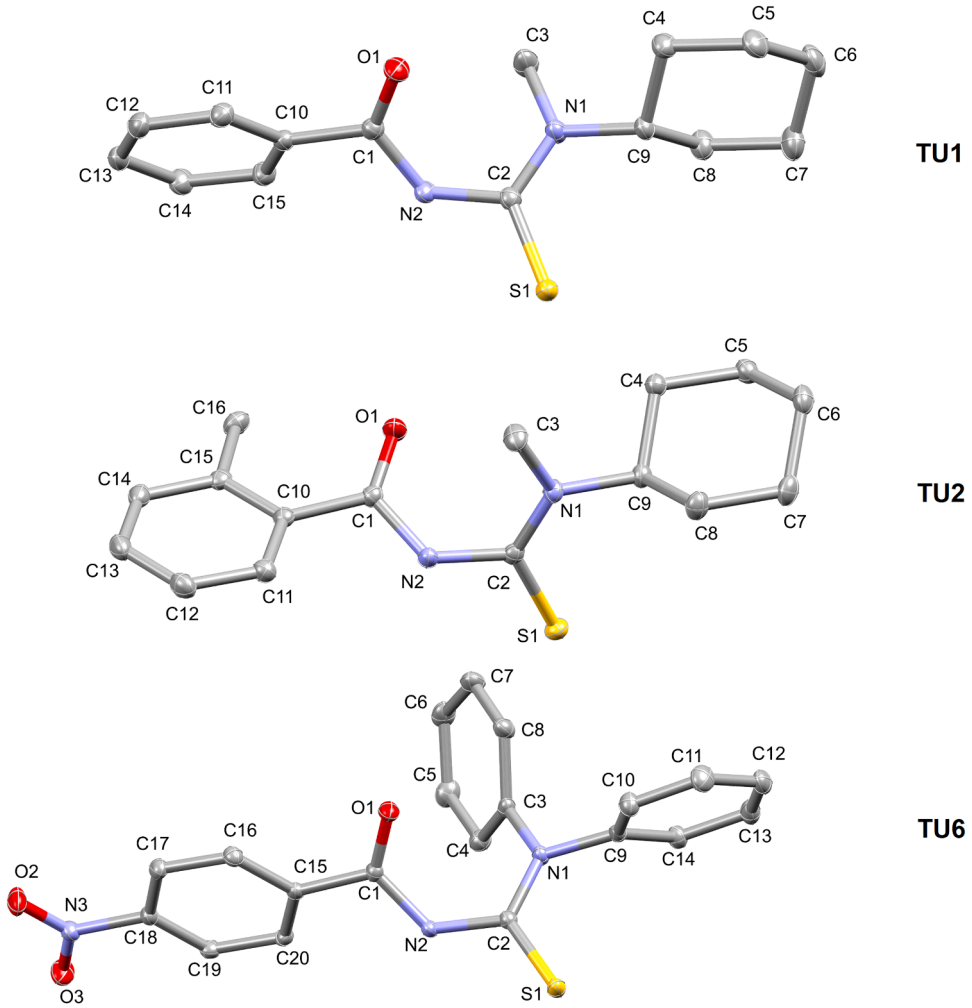

Fig. 2. Molecular structures of **TU1, TU2**, and **TU6**. Thermal ellipsoids are shown at a 50 % probability level, with hydrogen atoms removed for clarity.

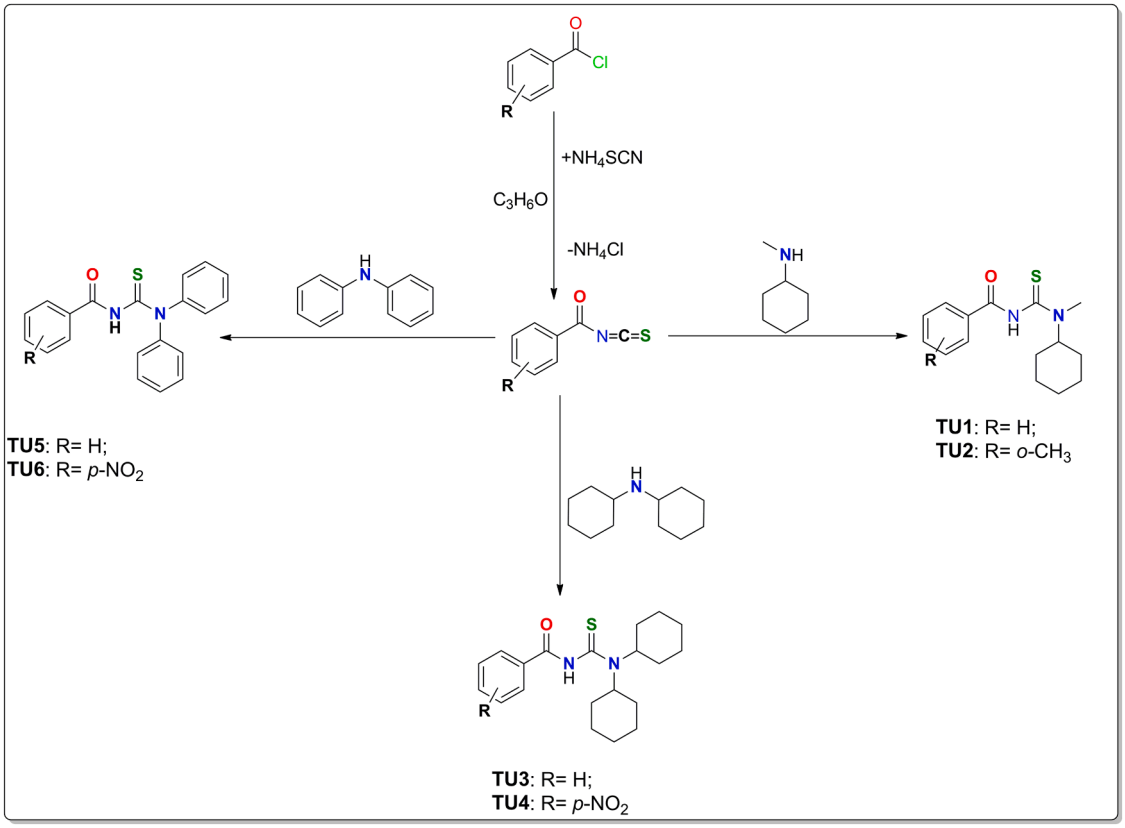

Scheme 1. Synthesis of thiourea ligands.

Table 2
Selected bond length and bond angles of **TU1, TU2** and **TU6**.

Bond length, Å	TU1	TU2	TU6
S1—C2	1.680(2)	1.677(11)	1.666(13)
O1—C1	1.216(2)	1.218(14)	1.214(18)
N1—C2	1.331(2)	1.328(14)	1.349(17)
N1—C3	1.465(3)	1.468(14)	1.448(17)
C1—N2	1.388(2)	1.385(14)	1.389(17)
C2—N2	1.401(2)	1.405(14)	1.395(16)
Bond angles, °			
C2—N1—C3	122.16(17)	122.65(10)	123.78(11)
O1—C1—N2	123.78(18)	121.75(11)	122.99(12)
N1—C2—N2	116.73(17)	116.51(10)	116.00(11)
N1—C2—S1	125.45(15)	125.90(9)	123.60(10)
N2—C2—S1	117.77(14)	117.58(8)	120.35(10)
C1—N2—C2	126.01(16)	124.91(10)	124.22(12)

correlates with reported structures ([46,47]). Table 3 shows the intramolecular and intermolecular hydrogen bonding of the compounds. **TU1** has one intramolecular hydrogen bond from C3—H3C···O1, ??? with a length of 2.852(2) Å and one intermolecular hydrogen bond from C3—H3B···O1 with a length of 3.216(3) Å. **TU2** has three intramolecular bonds from C3—H3B···O1, C3—H3C···N2 and C4—H4···S1 with a bond length of 2.8846(16) Å, 2.7586(16) Å and 3.0697(12) Å, respectively. The intramolecular hydrogen bonds in the structure form a 5-membered ring and a 7-membered ring structure. Furthermore, the structure is again stabilized by an intermolecular hydrogen bonding from N2—H2···S1 with a bond length of 3.3676(11) Å thus forming an 8-membered ring with S1, C1, N2, and H2 atoms of the molecule. **TU6** shows that the structure is stabilized by the intermolecular hydrogen bonding of the type N—H···S with distances of 3.3813(13) Å, thus forming an 8-membered ring with S1, C2, N2, and H2 atoms of the molecule resulting in dimer related by an inversion centre as shown in Figure S9.

3.2. FT-IR studies

The synthesized thiourea ligands show strong and broad absorption bands between 3350 and 3224 cm^{-1} attributed to the stretching vibration of ν(NH). The C—H stretching vibrations of the **TU1, TU2, TU3,**

Table 3
Summary of the hydrogen interaction bond lengths (Å) and angles () of the crystallized compounds.

Compound	D—H···A (Å)	D—H (Å)	H···A (Å)	D···A (Å)	D—H···A ()	Symmetry
TU1	C3—H3B···O1	0.98	2.58	3.216(3)	123	*1+x, y, z*
	C3—H3C···O1	0.98	2.06	2.852(3)	136	*x, y, z*
TU2	N2—H2···S1	0.88	2.68	3.3676(11)	136	*1-x, 1-y, 1-z*
	C3—H3B···O1	0.98	2.47	2.8846(16)	105	*x, y, z*
	C3—H3C···N2	0.98	2.39	2.7586(16)	102	*1-x, 1-y, 1-z*
	C4—H4···S1	1.00	2.55	3.0697(12)	112	*x, y, z*
TU6	N2—H2··· S1	0.88	2.56	3.3813(13)	156	*-x, 1-y, 1-z*
	C16—H16 ···O3	0.95	2.54	3.2357(19)	130	*1+x, y, z*
	C19—H19···O1	0.95	2.43	3.1591(17)	133	*1+x, y, z*

TU4, TU5 and **TU6** were observed in the 2978–2854 cm^{-1} range. The carbonyl group (C═O) stretching vibrations were observed as intense bands in the range 1690-1682 cm^{-1}. The bands observed in the 1290–1279 cm^{-1} range belong to C—N stretching vibrations. The C═C stretching vibrations of the aromatic rings were observed as multiple bands in the range of 1602–1560 cm^{-1}. The bands observed at 1540 and 1533 cm^{-1} on **TU4** and **TU6** are assign to asymmetric vibrations of Ar-NO_2, showing the substituent on the benzoyl ring. The symmetrical vibration observed at 1364 and1356 cm^{-1} are attributed to the *p*-NO_2 substituent on **TU4** and **TU6** respectively [48–52]. The IR spectra of the thiourea derivatives are given in Figure S1 and S2 (Supplemental Materials).

3.3. NMR studies

The ^{1}H and ^{13}C NMR data for the synthesized thiourea ligands were consistent with the proposed structures that were previously reported in the literature ([53,54]). The ^{1}H NMR spectrum of all ligands exhibited a singlet signal in the region of δ 9.99 and 8.03 ppm, which were assigned to the N-H proton. The multiplet signals ranging from δ 8-6 ppm were assigned to protons of an aromatic ring; slight variations were observed because of the difference in their chemical shifts. The most upfield protons in the ^{1}H NMR spectra of the ligands (**TU1, TU2, TU3,** and **TU4**) appeared as multiplet signals between δ 2.50-0.94 ppm, from the cyclohexyl group on the compounds. The other aliphatic protons signals (N-CH, N-CH_2) appeared downfield compared to the cyclohexyl signals as shown in Figures S3 and S4. Figure S5 and S6 showed the ^{13}C NMR spectrum of the synthesized compounds. The most de-shielded signals correspond to C═S and C═O groups. The C═S carbon atom for **TU1, TU2, TU3, TU4, TU5,** and **TU6** are δC = 181.2, 180.8, 182.4, 182.4, 182.2, and 184.2 ppm respectively. However, carbonyl group signals appeared at δC = 164.2, 166.3, 166.0, 166.0, 163.2, and 162.6 ppm for **TU1, TU2, TU3, TU4, TU5,** and **TU6**, respectively, due to the existence of intramolecular hydrogen bond interaction related to the carbonyl oxygen atom [55]. The formation of intramolecular hydrogen bonding increases the electronegativity of oxygen and sulphur atoms in different environments and conformations cause deshielding effects for these signals. Meanwhile, the aromatic carbon resonances were found between 120.1–146.3 ppm, corresponding to the benzene rings in the synthesized compounds.

3.4. In vitro antimycobacterial studies

The six compounds were subjected to *in-vitro* antimycobacterial screening against the H37RV *M. tuberculosis* strain using microbroth dilution assays. The 90 % Minimum Inhibitory Concentration (MIC_{90}) is defined as the lowest concentration of a compound required to inhibit 90 % of bacterial growth [56]. Table 4 displays the MIC_{90} values for the thiourea ligands and ethambutol, five of these compounds displayed activity against *M*tb. Compounds **TU1** and **TU2**, consisting of the monocyclohexyl group, were the most active among the tested compounds, with MIC_{90} of 28.3 and 11.3 μM, respectively. Compounds **TU4, TU5**, and **TU6**, which have MIC_{90} values of 80.3, 82.8 and 107.7 μM, respectively are considered to exhibit mild antituberculosis activity, whereas **TU3** with an MIC_{90} value of 752.7 μM is considered inactive. Based on the obtained results, it is evident that the different moieties brought about by the reacted secondary amines significantly influenced the antituberculosis activity, with the monocyclohexyl group being the most promising compared to the dicyclohexyl and diphenyl groups. Moreover, introducing the electron-donating *o*-methyl group in **TU2** appears beneficial compared to the electron-withdrawing *p*-NO_2 group in **TU4** and **TU6**. Dogan and co-workers synthesized *N*-pyridine-*N*′-aryl thiourea derivatives introducing (substituted) phenyl/naphthyl rings into the structure of the compounds. Based on the results derived from the investigation, it was observed that two compounds, which underwent halogen and nitro group substitutions, had reasonable efficacy as antimycobacterial agents. These compounds demonstrated a MIC value ≤ 1.56 μM, distinguishing them from the remaining derivatives. In addition, it was observed that the activity of the compounds was comparable to that of Ethambutol (7.6 μM), which served as a reference standard. The addition of chlorine, bromine, iodine, and nitro atoms resulted in a significant reduction in the MIC values as compared to unsubstituted phenyl/naphthyl. Moreover, the absence of substitutions on the phenyl/naphthyl ring resulted in the loss of the compounds' antitubercular efficacy [57,58].

Table 4
MIC_{90} values of antimycobacterial activity of thiourea ligands and the IC_{50} data of cervical cancer (HeLa) and breast epithelial cells (MCF12A).

Compounds	MIC (μg/mL)	MIC (μM)	HeLa (μM) SI	MCF12A (μM) SI
TU1	7.80	28.26	36.89 ± 1.23 1.30	11.62 ± 1.16 0.41
TU2	3.90	11.33	12.00 ± 1.21 1.06	9.34 ± 1.14 0.82
TU3	250	752.76	71.73 ± 1.38 0.10	44.95 ± 1.21 0.06
TU4	31.25	80.30	27.75 ± 1.15 0.35	45.71 ± 1.21 0.57
TU5	31.25	82.87	23.66 ± 1.24 0.29	60.80 ± 1.23 0.73
TU6	31.25	107.70	8.45 ± 1.21 0.08	2.49 ± 1.23 0.02
Ethambutol	1.95	9.56		

*SI = selectivity index

3.5. In vitro anticancer studies

The IC_{50} or half-maximal inhibitory concentration, values were calculated to evaluate the toxicity of the compounds studied against human cells and to predict their therapeutic potential (see Table 4). The compounds, **TU1, TU2, TU3, TU4, TU5** and **TU6** displayed IC_{50} values of 36.89, 12.0, 71.76, 27.75, 23.66 and 8.45 μM, respectively against HeLa cell lines and 11.62, 9.34, 44.95, 45.71, 60.80 and 2.49 μM, respectively against the MCF12A. Overall, the compounds were not selective for *Mtb* over either of the human cell lines, as indicated by selectivity indices of < 1 in most cases. Only **TU1** and **TU2** displayed SI values greater than 1 in HeLa cells (1.3 and 1.06). **TU3** and **TU6**, on the other hand, were significantly (>10x) more toxic to human cells than *Mtb* bacterial cells (SI = 0.10 and 0.06 for **TU3** in HeLa and MCF12A, respectively, and 0.08 and 0.02 for **TU6** in HeLa and MCF12A, respectively). The results reveal that **TU1** and **TU2**, the most potent against *Mtb*, are also toxic to human cells and the concentrations used to achieve 90 % inhibition of *Mtb* would result in approximately 50 % inhibition of human cells.

4. Conclusion

All the compounds were synthesized and obtained with a high degree of purity and yields using a straightforward synthetic methodology. The synthesized compounds showed similar structural parameters with other comparable thiourea derivatives. The molecules were linked together through intermolecular hydrogen bonds, specifically N—H···S and C—H···O interactions. Given the significant global mortality caused by tuberculosis, the identification and development of novel drugs exhibiting unique structural and mechanistic characteristics is paramount. The influence of the molecular structure on the microbial activity of the compounds was noted, with the compounds containing the monocyclohexyl group being more active than those with dicyclohexyl and diphenyl groups. In addition, the compound possessing the electron-donating *o*-methyl group on the benzoyl ring exhibited significant antimicrobial properties compared to those with the electron-withdrawing *p*-NO_2 group. Thus, compounds **TU1** and **TU2** offer the

most promise and may be used as hit compounds in designing more efficacious and selective derivates.

CRediT authorship contribution statement

Luleka Makhakhayi: Writing – original draft, Methodology, Data curation. **Frederick P. Malan:** Writing – original draft, Data curation. **Sibusiso Senzani:** Methodology, Data curation. **Matshawandile Tukulula:** Writing – review & editing, Methodology, Data curation. **Candace Davison:** Methodology, Data curation. **Jo-Anne de la Mare:** Writing – review & editing, Methodology, Data curation. **Comfort M. Nkambule:** Writing – review & editing, Supervision, Methodology. **Vuyelwa J. Tembu:** Writing – review & editing, Supervision. **Amanda-Lee E. Manicum:** Supervision, Conceptualization, Methodology, Writing – review & editing.

Declaration of competing interest

The authors declare no conflicts of interest regarding this article.

Data availability

Data will be made available on request.

Acknowledgements

We greatly acknowledge the strong guidance, motivation, and support provided by the individual authors. We would like to thank the National Research Foundation of South Africa (Grant No. 129468 (AEM); Grant No. 117898 (VJT) grant No. TTK190403426633 (JdlM)), Tshwane University of Technology (AEM, VJT), the University of Pretoria and Rhodes University (JdlM) for institutional and financial support. The authors would like to express their gratitude towards NCP Chlorchem for financial assistance.

Supplementary materials

Supplementary material associated with this article can be found, in the online version, at doi:10.1016/j.molstruc.2024.138818.

References

[1] A. Arslan, N. Duran, G. Borekci, C.K. Ozer, C. Akbay, Antimicrobial activity of some thiourea derivatives and their nickel and Copper complexes, Molecules 14 (2009) 519–527, https://doi.org/10.3390/molecules14010519.
[2] L. Makhakhayi, F.P. Malan, V.J. Tembu, C.M. Nkambule, A. Manicum, The crystal structure of *fac*-tricarbonyl(N-benzoyl-*N,N*-cyclohexylmethylcarbamimidothioato-κ2S,O-pyridine-κN)rhenium(I), $C_{23}H_{24}N_3O_4ReS$, Z. Kristallogr. 238 (2023) 697–699, https://doi.org/10.1515/ncrs-2023-0157.
[3] W.K. Komane, P. Mokolokolo, B. Vatsha, A. Manicum, The crystal structure of *fac*-tricarbonyl (*N'*-benzoyl-*N,N*-diphenylcarbamimidothioato-κ2S,O-pyrazole-κ*N*) rhenium(I)-methanol(1/1) C26H23O4N4SRe, Z. Kristallogr. 236 (2021) 767–769, https://doi.org/10.1515/ncrs-2021-0046.
[4] N.Kumar Singh, S. Shrestha, N. Shahi, R.A. Kumar Choudhary, A. Kumbhar, Y. R. Pokharel, P. Nath Yadav, Enhancement of anticancer activity of N(4)1-(2-pyridyl)piperazinyl 5-nitroisatin thiosemicarbazone on chelation with Copper(II), Asian. J. Chem. 33 (2021) 557–564, https://doi.org/10.14233/ajchem.2021.23004.
[5] P. Cui, X. Li, M. Zhu, B. Wang, J. Liu, H. Chen, Design, synthesis and antibacterial activities of thiouracil derivatives containing acyl thiourea as SecA inhibitors, Bioorg. Med. Chem. Lett. 27 (2017) 2234–2237, https://doi.org/10.1016/j.bmcl.2016.11.060.
[6] M. Marzi, K. Pourshamsian, F. Hatamjafari, A. Shiroudi, A.R. Oliaey, Synthesis of New *N*-benzoyl-*N'*-triazine thiourea derivatives and their antibacterial activity, Russ. J. Bioorg. Chem. 45 (2019) 391–397, https://doi.org/10.1134/S106816201905008X.
[7] E. Khan, S. Khan, Z. Gul, M. Muhammad, Medicinal importance, coordination chemistry with selected metals (Cu, Ag, Au) and chemosensing of thiourea derivatives, Crit. Rev. Anal. Chem. 51 (2021) 812–834, https://doi.org/10.1080/10408347.2020.1777523.
[8] R.K. Mohapatra, P.K. Das, M.K. Pradhan, M.M. El-Ajaily, D. Das, H.F. Salem, M. K. E-Zahan, Recent advances in urea-and thiourea-based metal complexes: biological, sensor, optical, and corrosion inhibition studies, Comments Inorg. Chem. 39 (2019) 127–187, https://doi.org/10.1080/02603594.2019.1594204.
[9] V. Citi, A. Martelli, M. Bucci, E. Piragine, L. Testai, V. Vellecco, V. Calderone, Searching for novel hydrogen sulfide donors: the vascular effects of two thiourea derivatives, Pharmacol. Res. Commun. 159 (2020) 105039–105069, https://doi.org/10.1016/j.phrs.2020.105039.
[10] B. Shakya, N. Shahi, F. Ahmad, P.N. Yadav, Y.K Pokharel, 2-Pyridineformamide N (4)-ring incorporated thiosemicarbazones inhibit MCF-7 cells by inhibiting JNK pathway, Bioorg. Med. Chem. Lett. 29 (2019) 1677–1681, https://doi.org/10.1016/j.bmcl.2019.04.031.
[11] W.A.A. Arafa, A.A. Ghoneim, A.K. Mourad, *N*-Naphthoyl Thiourea derivatives: An efficient ultrasonic-Assisted synthesis, reaction, and *in-vitro* anticancer evaluations, ACS Omega 7 (2022) 6210–6222, https://doi.org/10.1021/acsomega.1c06718.
[12] O. Özbek, M.B. Gürdere, A review on the synthesis and applications of molecules as anticonvulsant drug agent candidates, Med. Chem. Res. 29 (2020) 1553–1578. https://link.springer.com/article/10.1007/s00044-020-02595-4.
[13] M. Tapera, H. Kekeçmuhammed, K. Sahin, V.S. Krishna, C. Lherbet, H. Homberset, E. Sarıpınar, Synthesis, characterization, anti-tuberculosis activity and molecular modeling studies of thiourea derivatives bearing aminoguanidine moiety, J. Mol. Struct. 1270 (2022) 133899–133942, https://doi.org/10.1016/j.molstruc.2022.133899.
[14] M.G. Moule, J.D. Cirillo, Mycobacterium tuberculosis dissemination plays a critical role in pathogenesis, Front. Cell. Infect. Microbiol. 10 (2020) 1–12, https://doi.org/10.3389/fcimb.2020.00065.
[15] S.K. Sharma, A. Mohan, A. Sharma, D.K. Mitra, Miliary tuberculosis: new insights into an old disease, Lancet Infect. Dis. 5 (2005) 415–430, https://doi.org/10.1016/S1473-3099(05)70163-8.
[16] I. Smith, Mycobacterium tuberculosis pathogenesis and molecular determinants of virulence, Clin. Microbiol. Rev. 16 (2003) 463–496, https://doi.org/10.1128/CMR.16.3.463-496.2003.
[17] D.R. Silva, F.C.Q. Mello, G.B. Migliori, Diagnosis and management of post-tuberculosis lung disease, J. Bras. Pneumol. 49 (2023) 55–56, https://doi.org/10.36416/1806-3756/e20230055.
[18] S. Goverdhan, K.M. Sandeep, Y. Perumal, S. Dharmarajan, K. Srinivas, Dibenzofuran, dibenzothiophene and *N*-methyl carbazole tethered 2-aminothiazoles and their cinnamamides as potent inhibitors of *Mycobacterium* tuberculosis, Bioorganic. Med. Chem. Lett. 28 (2018) 1610–1614, https://doi.org/10.1016/j.bmcl.2018.03.048.
[19] S. Selvaraju, K. Thiruvengadam, B. Watson, N. Thirumalai, M. Malaisamy, C. Vedachalam, S. Swaminathan, C. Padmapriyadarsini, Long-term survival of treated tuberculosis patients in comparison to a general population In South India: a Matched cohort study, Int. J. Infect. Dis. 110 (2021) 385–393, https://doi.org/10.1016/j.ijid.2021.07.067.
[20] V.A. Dartois, E.J. Rubin, Anti-tuberculosis treatment strategies and drug development: challenges and priorities, Nat. Rev. Microbiol. 20 (2022) 685–701, https://doi.org/10.1038/s41579-022-00731-y.
[21] E. Tatar, S. Karakuas S.G. Küçükgüzel, S.O. Okullu, N. Ünübol, T. Kocagöz, E. De Clercq, G. Andrei, R. Snoeck, C. Pannecouque, S. Kalaycı, F. Sahin, D. Sriram, P. Yogeeswari, I. Kücükgüzel, Design, synthesis, and molecular docking studies of a conjugated thiadiazole–thiourea scaffold as antituberculosis agents, Biol. Pharm. Bull. 39 (2016) 502–515, https://doi.org/10.1248/bpb.b15-00698.
[22] N.A. Meanwell, Synopsis of some recent tactical application of bioisosteres in drug design, J. Med. Chem. 54 (2011) 2529–2591, https://doi.org/10.1021/jm1013693.
[23] V. Kumar, S. Chimni, Recent developments on thiourea based anticancer chemotherapeutics, Anticancer Agents Med. Chem. 15 (2015) 163–175, https://doi.org/10.2174/1871520614666140407123526.
[24] K.N. Venugopala, M. Kandeel, M. Pillay, P.K. Deb, H.H. Abdallah, M. F. Mahomoodally, D. Chopra, Anti-tubercular properties of 4-Amino-5-(4-fluoro-3-phenoxyphenyl)-4H-1,2,4-triazole-3-thiol and Its Schiff bases: computational input and molecular dynamics, J. Antibiot. 9 (2020) 559–575, https://doi.org/10.3390/antibiotics9090559.
[25] E. Cox, K. Laessig, FDA Approval of Bedaquiline—The benefit–risk balance for drug-resistant tuberculosis, N. Engl. J. Med. 371 (2014) 689–691, https://doi.org/10.1056/NEJMp1314385.
[26] C.E. Barry, Timing is everything for compassionate use of delamanid, Nat. Med. 21 (2015) 211–212, https://doi.org/10.1038/nm.3823.
[27] I.B. Douglass, F.B. Dains, Some derivatives of benzoyl and furoyl isothiocyanates and their use in synthesizing heterocyclic compounds, J. Am. Chem. Soc. 56 (1934) (1934) 719–721, https://doi.org/10.1021/ja01318a057.
[28] S. Warsink, P.D. Riekert Kotze, J.M. Janse van Rensburg, J.A. Venter, S. Otto, E. Botha A. Roodt, Kinetic-mechanistic and Solid-State study of the oxidative addition and migratory insertion of iodomethane to [Rhodium(*S,O*-BdiPT or N,O-ox)(CO)($PR^1R^2R^3$)] complexes, Eur. J. Inorg. Chem. (2018) 3615–3625, https://doi.org/10.1002/ejic.201800293.
[29] Rigaku Oxford Diffraction, CrysAlisPro Software system, (2018).
[30] G.M. Sheldrick, SHELXT integrated space-group and crystal-structure determination, Acta Crystallogr. A71 (2015) 3–8, https://doi.org/10.1107/S2053273314026370.
[31] O.V. Dolomanov, L.J. Bourhis, R.J. Gildea, J.A.K. Howard, H. Puschmann, OLEX2: a complete structure solution, refinement and analysis program, J. Appl. Crystallogr. 42 (2009) 339–341, https://doi.org/10.1107/S0021889808042726.
[32] W. Pennington, DIAMOND - visual crystal structure information system, J. Appl. Crystallogr. 32 (1999) 1028–1029, https://doi.org/10.1107/S0021889899011486.

[33] C.F. Macrae, I.J. Bruno, J.A. Chisholm, P.R. Edgington, P. McCabe, E. Pidcock, L. Rodriguez-Monge, R. Taylor, J. Van de Streek, P.A. Wood, New features for the visualization and investigation of crystal structures, J. Appl. Crystallogr. 41 (2008) 466–470, https://doi.org/10.1107/s1600576719014092.
[34] N.T.P. Nyoni, N.B. Ncube, M.X. Kubheka, N.P. Mkhwanazi, S. Senzani, T. Singh, M. Tukulula, Synthesis, characterization, in vitro antimycobacterial and cytotoxicity evaluation, DFT calculations, molecular docking and ADME studies of new isomeric benzimidazole-1,2,3-triazole-quinoline hybrid mixtures, Bioorg. Chem. 141 (2023) 106904–106921, https://doi.org/10.1016/j.bioorg.2023.106904.
[35] M. Mbaba, L.M.K. Dingle, D. Cash, J.-A.D.L. Mare, D. Laming, D. Taylor, H. C. Hoppe, A.L.K. Edkins, S.D. Khanye, Repurposing a polymer precursor: Synthesis and *in-vitro* medicinal potential of ferrocenyl 1,3-benzoxazine derivatives, Eur. J. Med. Chem. 187 (2020) 111924–111981, https://doi.org/10.1016/j.ejmech.2019.111924.
[36] M. Mbaba, J.A. de la Mare, J.N. Sterrenberg, D. Kajewole, S. Maharaj, A.L. Edkins, M. Isaacs, H.C. Hoppe, S.D. Khanye, Novobiocin-ferrocene conjugates possessing anticancer and antiplasmodial activity independent of HSP90 inhibition, J. Biol. Inorg. Chem. 24 (2019) 139–149, https://doi.org/10.1007/s00775-018-1634-9.
[37] G. Binzet, G. kavak, N. Kulcu, S. Ozbey, U. Florke, H. Arslan, Synthesis and characterization of novel thiourea derivatives and their nickel and copper complexes, J. Chem. 10 (2013) 1–9, https://doi.org/10.1155/2013/536562.
[38] G. Binzet, U. Flörke, N. Külcü, H. Arslan, Crystal structure of 3-(2-chlorobenzoyl)-1.1-diphenylthiourea, (C6H5)2N(CS)(NH)(CO)(C6H4Cl), Z. Kristallogr. 219 (2004) 395–397, https://doi.org/10.1524/ncrs.2004.219.14.427.
[39] A. Saeed, U. Flörke, (1-(2-Nitrophenyl)-3-pivaloythiourea), Acta Crystallogr. 63 (2007), https://doi.org/10.1107/S160053680704593X, 04259-04259.
[40] A. Saeed, M. Parvez, The crystal structure of 1-(4-chlorophenyl)-3-(4-methylbenzoyl) thiourea, Cent, Eur. J. Chem. 3 (2005) 780–791, https://doi.org/10.2478/BF02475204.
[41] R.D. Campo, J.J. Criado, R. Gheorghe, F.J. Gonzalez, M.R. Hermosa, F. Sanz, J. L. Manzano, E. Monte, E. Rodriguez-Fernandez, *N*-benzoyl-N-allylthiourea and their complexes with Ni (II), Co (III) and Pt (II)—crystal structure of 3-benzoyl-1-butyl-1-methylthiourea: activity against fungi and yeast, J. Inorg. Biochem. 98 (2004) 1307–1314, https://doi.org/10.1016/j.jinorgbio.2004.03.019.
[42] G. Binzet, U. Flörke, N. Külcü, H. Arslan, Crystal and molecular structure of bis(4-bromo-N-(diethylcarbamothioyl) benzamido) nickel (II) complex, Eur. J. Chem. 3 (2012) 37–39, https://doi.org/10.5155/eurjchem.3.2.211-213.594.
[43] B. Yamin, S. Yousuf, M. mohd yusof, T. Zakaria, 1-(2-Methyl-benzo-yl)-3-m-tolyl-thio-urea, Acta Crystallogr. Section E, Struct. Rep. online 64 (2008), https://doi.org/10.1107/S1600536808012300 o1227-o1227.
[44] W. Yang, W. Zhou, Z. Zhang, Structural and spectroscopic study on N-2-fluorobenzoyl-N-4-methoxyphenylthiourea, J. Mol. Struct. 828 (2007) 46–53, https://doi.org/10.1016/j.molstruc.2006.05.033.
[45] H. Arslan, U. Flörke, N. Kulcu, The crystal and molecular structure of 1-(2-chlorobenzoyl)-3-p-tolyl-thiourea, Turk. J. Chem. 28 (2004) 673–678. https://journals.tubitak.gov.tr/chem/vol28/iss6/1.
[46] J.R. Sabino, S. Cunha, R.M. Bastos, I. Vencato, N- (benzylaminothiocarbonyl) benzamide, Acta Crystallogr. 62 (2006) o3918–o3920, https://doi.org/10.1107/S1600536806031928.
[47] S. Saeed, N. Rashid, A. Muhammad, H. Rizwan, P. Jones, Synthesis, spectroscopic characterization, crystal structure and pharmacological properties of some novel thiophene-thiourea core derivatives, Eur. J. Chem. 3 (2010) 221–227, https://doi.org/10.5155/eurjchem.1.3.221-227.124.
[48] R. Sajidur, A. Saeed, G. Saddique, P.A. Channar, F.A. Larik, Q. Abbas, M. Hassan, H. Raza, T.A. Fattah, S.Y. Seo, Synthesis of sulfadiazinyl acyl/aryl thiourea derivatives as calf intestinal alkaline phosphatase inhibitors, pharmacokinetic properties, lead optimization, Lineweaver-Burk plot evaluation and binding analysis, Bioorg. Med. Chem. 23 (2018) 3707–3715, https://doi.org/10.1016/j.bmc.2018.06.002.
[49] X. Zhang, X. Du, J. Song, J. Huang, Synthesis, crystal structure, hydrogen bonding interactions analysis of novel acyl thiourea derivative, J. Phys .Org. Chem. 33 (2019) 4016–4025, https://doi.org/10.1002/poc.4016.
[50] X. Zhang, J. Huang, Y. Zhang, F. Qi, S. Wang, J. Song, Synthesis, crystal structure and non-covalent interactions analysis of novel N-substituted thiosemicarbazone, Chem. Res. Chin. Univ. 35 (2019) 471–477, https://doi.org/10.1007/s40242-019-8354-8.
[51] M.K. Rauf, S. Zaib, A. Talib, A. Ebihara, A. Badshah, M. Bolte, J. Iqbal, Bioorg. Med. Chem. Lett. 24 (2016) 4452–4463, https://doi.org/10.1016/j.bmc.2016.07.042.
[52] A. Bielenica, J. Stefanska, K. Stepien, A. Napiorkowska, E. Augustynowicz-Kopec, G. Sanna, S. Madeddu, S. Boi, G. Giliberti, M. Wrzosek, M. Struga, Synthesis, cytotoxicity and antimicrobial activity of thiourea derivatives incorporating 3-(trifluoromethyl)phenyl moiety, Eur. J. Med. Chem. 101 (2015) 111–125, https://doi.org/10.1016/j.ejmech.2015.06.027.
[53] G. Binzet, H. Arslan, U. Flörke, N. Külcü, N. Duran, Synthesis, characterization, and antimicrobial activities of transition metals complexes with *N, N*-dialkyl-*N*'(2-chlorobenzoyl) thiourea derivatives, J. Coord. Chem. 59 (2006) 1395–1406, https://doi.org/10.1080/00958970500512633.
[54] H. Arslan, N. Kulcu, U. Florke, Synthesis and characterization of copper(II), nickel (II) and cobalt(II) complexes with novel thiourea derivatives, Transit. Metal Chem. 28 (2003) 816–819. http://doi.org/10.1023/A:1026064232260.
[55] F. Adam, N.N. Fatihah, N. Ameram, S. Subramaniam, S.A. Mubarrakh, The synthesis and characterisation of 2-methyl-N-((4-methylpyridine-2-yl)carbamothiol)benzamide: Its preparation with antibacterial study, J. Phys. Sci. 27 (2016) 83–101, https://doi.org/10.21315/jps2016.27.2.7.
[56] B. Kowalska-Krochmal, R. Dudek-Wicher, The minimum inhibitory concentration of antibiotics: methods, interpretation, clinical relevance, J. Pathog. 10 (2021) 165–185, https://doi.org/10.3390/pathogens10020165.
[57] S.D. Dogan, M.G. Gunduz, H. Dogan, S.K. Vagolu, L. Christian, D. Sriram, Design and synthesis of thiourea-based derivatives as Mycobacterium tuberculosis growth and enoyl acyl carrier protein reductase (InhA) inhibitors, Eur. J. Med. Chem. 199 (2020) 112402–112432, https://doi.org/10.1016/j.ejmech.2020.112402.
[58] M. Singh, P. Sasi, G. Rai, V.H. Gupta, D. Amarapurkar, P.P. Wangikar, Studies on toxicity of antitubercular drugs namely isoniazid, rifampicin, and pyrazinamide in an in vitro model of HepG2 cell line, Med. Chem. Res. 20 (2011) 1611–1615, https://doi.org/10.1007/s00044-010-9405-3.